Enhanced Cellular Functions on Polycaprolactone Tissue Scaffolds by O_2 Plasma Surface Modification

Eda D. Yildirim, Daphne Pappas, Selçuk Güçeri, Wei Sun*

This paper reports a study of using an oxygen-based plasma modification to alter physicochemical properties of three-dimensional (3D) PCL scaffolds and to improve mouse osteoblast cells attachment, proliferation, and osteoblastic differentiation. Different plasma modification times (1, 3, and 5-min) and their effects on surface physicochemical properties were measured by contact angle measurement, surface energy calculation (Owens–Wendth Method), surface chemistry (XPS), and the surface topography (AFM). The effect of oxygen-based plasma modification on attachment, proliferation, and osteoblastic differentiation were examined by shear flow assay, alamarBlue assay, scanning electron microscopy (SEM), and osteoblastic differentiation markers. Results of the contact angle measurement, total solid surface energy, surface chemistry, and roughness revealed that oxygen-based plasma modification increased surface hydrophilicity, total surface energy, total amount of oxygen containing groups, and the surface roughness. A positive effect of plasma modification on cell proliferation on 3D PCL scaffolds was observed at the osteoblastic differentiation stage which was evaluated by the alkaline phosphatase (ALP) activity, osteocalcin protein secretion, and calcium mineralization. The higher ALP activity and osteocalcin secretion were detected from the cells on 3-min plasma modified PCL surface compared to unmodified samples. The calcium mineralization and SEM micrographs data also showed that there was a higher mineralized matrix deposition on 3-min plasma modified PCL scaffolds compared to unmodified scaffolds. These results suggest that the 3-min plasma modification can accelerate differentiation phase of osteoblast through improving cell–scaffold interaction.

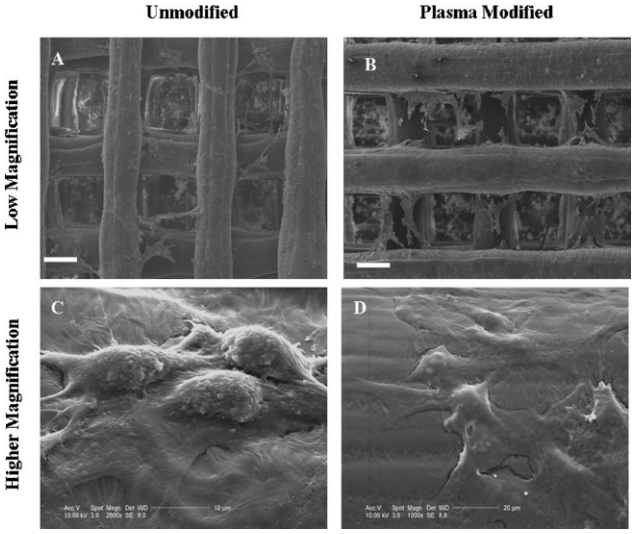

E. D. Yildirim, S. Güçeri, W. Sun
Department of Mechanical Engineering and Mechanics, Drexel University, 3141 Chestnut Street, Philadelphia, Pennsylvania 19104, USA
Fax: +1 215 895 1478; E-mail: sunwei@drexel.edu
D. Pappas
Army Research Laboratory, Aberdeen Proving Ground, Maryland 21005, USA

Introduction

Three-dimensional (3D) tissue scaffolds play a vital role in tissue engineering because it can serve as pre-formed extracellular matrices (ECM) onto which cells can attach, grow, and form new tissues.[1,2] In the orchestrated process of tissue regeneration, cells are significantly influenced by the

DOI: 10.1002/ppap.201000009

structural and chemical cues provided by the micro-architecture of 3D scaffolds for their proliferation, migration, and differentiation.[3–6] Most enabling bio-additive manufacturing techniques can produce 3D scaffolds with designed geometry and internal architectures.[2,7–11] However those fabricated scaffolds often do not possess the desired surface chemical cue to stimulate tissue regeneration.[12–14] For example, Polycaprolactone (PCL) has been found as an ideal biopolymer in bone tissue engineering and drug delivery application due to its biocompatible, structural stability, and long degradation properties;[15] however, low surface energy and the absence of bioactive functional groups on PCL surface create an interference with cell affinity and the subsequent cellular interaction for tissue regeneration within the PCL scaffolds.[16] To enhance bioactive properties on PCL surface, there are various surface modification techniques reported in the open literature, including chemical treatment,[17] blending,[18] laser surface modification,[19] ion beam radiation,[20] and plasma modification.[21–22] Among them, plasma surface modification technique has the advantage of altering the surface properties without changing the bulk behavior of the treated PCL substrates. Plasma modification also has advantages of free of residual solvents on the substrate surface in contrast to wet chemical surface modification techniques.[23]

This paper will report our current study on using plasma surface modification technique to enhance the cell attachment, proliferation, and differentiation on 3D PCL tissue scaffolds. The fabrication and plasma induced surface modification of 3D PCL scaffolds will be first described. The plasma modification induced changes in surface physico-chemical properties will be discussed after measuring surface hydrophilicity, solid surface energy, surface chemistry, and surface topography. Then 21 d cell culture study will be explained to investigate the effect of the plasma treatment on long-term osteoblast cellular functions and differentiation within 3D PCL scaffolds. The changes in cellular activity on PCL scaffolds as a result of plasma exposure will be evaluated through the measurement of cell adhesion strength and the metabolic activity by using shear flow assay and alamarBlue (aB) assay, respectively. The differentiation rate of osteoblast on 3D plasma modified PCL scaffolds will be quantified by measuring the production of alkaline phosphatase (ALP) activity, secretion of osteocalcin and mineralization of calcium.

Experimental Part

Fabrication of Three Dimensional Polycaprolactone (PCL) Scaffolds

In this study, the 3D PCL scaffolds were fabricated by an additive manufacturing based precision extrusion deposition (PED) system.[9,10,24] Poly ε-caprolactone (PCL, Sigma Aldrich Inc, MO, USA) in the form of pellets was used as scaffolding material. PCL has a molecular weight of 42 500 (Mn) and a melt index of 1.9g/10 min (ASTM D-1238-73). It has a low glass transition temperature at −60 °C, a melting temperature at about 58–60 °C, and a high thermal stability. The fabricated 3D scaffold has a geometry in $6 \times 6 \times 2\ mm^3$ with a 0°/90° strut layout pattern. It contains 18 layers of 300 μm pore size and 250 μm strut width. Following the fabrication process, all scaffolds were sterilized by submerging them inside 70% ethanol over night under sterile laminar hood until the plasma modification.

Polycaprolactone (PCL) Scaffold Surface Modification

The sterile PCL scaffolds were modified with a plasma reactor (PDC 32G, Harrick Scientific Inc., New York). The plasma reactor consists of a helical internal electrode around the plasma chamber with integrated gas feeding and vacuum pumping system (Figure 1). The PCL scaffolds were placed in the plasma chamber and oxygen (O_2) was purged to the chamber at flow rate of 1 SLPM by integrated gas feeding system. Throughout the treatment the chamber was kept at low pressure (~200 mTorr) through vacuum pump with pumping speed $6\ m^3 \cdot h^{-1}$. Then, 100 W of radio-frequency (RF 13.56 MHz) power was applied to create high-frequency magnetic field being able to provide breakdown and sustain the plasma. The plasma generated in this way modified the 3D PCL scaffold surface evenly for 1, 3, and 5 min exposure period. After the plasma modification, the samples were transferred to a laminar air flow biological safety cabinet for further cell function study.

Characterization of the Surface Properties

Assessment of Surface Hydrophilicity and Solid Surface Energy

The assessment of hydrophilicity for PCL before and after plasma exposure was done by series of contact angle measurements on non porous, flat-surfaced PCL films. The films were prepared by a melting process during which PCL pellets were heated at 90 °C, the scaffolds' extrusion temperature. The contact angle (θ) of probe liquids (diiodomethane, ultra pure water, and glycerol) on treated and untreated PCL surfaces were measured by sessile drop technique. In this technique, a drop of probe liquid (2 μL) was placed onto PCL surface and then the contact angle was measured from the drop profile. The angle measurements were taken at least four times and an average value was calculated. All contact angle measurements were done at room temperature by commercial contact angle measurement device, KSV Instruments CAM 200.

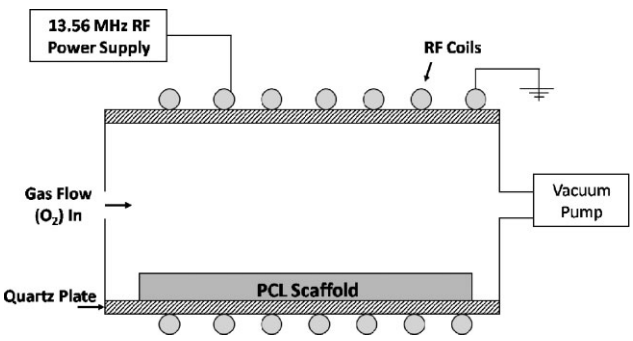

Figure 1. Schematic of plasma reactor.

DOI: 10.1002/ppap.201000009

The contact angle data then used for calculating solid surface energy based on Young's equation.

$$\sigma_s = \gamma_{sl} + \sigma_l \cdot \cos\theta \quad (1)$$

In above equation, however there are two unknown namely solid surface energy (σ_s) and solid/liquid interfacial energy (γ_{sl}). In order to eliminate the γ_{sl} the Owens–Wendt's method was used. In Owens–Wendt's method, the surface tension of liquid and solid phase can be split into dispersion component (σ^D) and polar component (σ^P).

$$\sigma_l = \sigma_l^P + \sigma_l^D \quad \sigma_s = \sigma_s^P + \sigma_s^D \quad (2)$$

where superscripts D and P represent the dispersive and polar components respectively whereas subscripts s and l denote solid and liquid phases, respectively. The solid surface energy is the summation of its polar and dispersive components. The solid/liquid interfacial energy (γ_{sl}) was written in the form of dispersive and polar component of solid and liquid surface energy.

$$\gamma_{sl} = \sigma_s + \sigma_l - \left(\frac{4\sigma_l^D\sigma_s^D}{\sigma_l^D + \sigma_s^D} + \frac{4\sigma_l^P\sigma_s^P}{\sigma_l^P + \sigma_s^P}\right) \quad (3)$$

It is possible to calculate the polar and disperse fractions of the surface energy with the aid of a single linear regression from the contact angle data of various liquids.[21]

Assessment of Surface Chemistry and Topography

X-ray photoelectron spectroscopy (XPS, Axis Ultra 165, Kratos-Shimadzu Corporation, USA) was used to identify changes in near surface compositional depth profiling for modified and unmodified PCL samples. Spectra were obtained by Kratos Axis Ultra 165 spectrometer using A1K$_\alpha$ (1486.7 eV) beam radiation at a power of 100 W. A take-off angle of 90° with respect to the $1 \times 0.5\,mm^2$ sampling area was used. All measurements were taken under vacuum between 10^{-9} and 10^{-10} Torr. Elemental high resolution scans for C1s, O1s, Si2s, Si2p, and N1s were taken at the pass energy of 20 eV. A value of 285.0 eV for the hydrocarbon C1s core level was used as the calibration energy for the binding energy scale.

Atomic force microscopy (AFM, 3100 AFM, Digital Instruments, USA) was used to evaluate surface topography on PCL in terms of surface features and surface roughness. A Dimension 3100 AFM (Digital Instruments, USA) was used in tapping mode at ambient conditions. The scan size was 5 μm. Samples were scanned at a frequency of 1 Hz. Nanoscope 5.12 software was utilized to determine surface characteristics from AFM image data. In order to remove the artifacts such as artificial curvatures, tilt, and distortion, all images were subjected to a third order flatten using the Nanoscope software. Root-mean-square roughness (RRMS) which is the standard deviation from the mean surface level of the image was measured by Nanocope software. In addition, phase AFM images of PCL film surface over a $5 \times 5\,\mu m^2$ square were plotted.

Assessment of Cell–Scaffold Interaction

To evaluate the effect of plasma modification on the cell–scaffold interaction 7F2 mouse osteoblast cells (CRL-12557, American Type. Culture Collection, Rockville, MD) with a passage number 23–30 were used. The cells were cultured in alpha-minimum essential medium (α-MEM) (Gibco, NY) containing 10% fetal bovine serum (Hyclone, UT), 2 mM L-glutamine and 1 mM sodium pyruvate without ribonucleosides and deoxyribonucleosides at incubator condition (37 °C and 5% CO_2). Beginning from the third day of the culture, the medium was supplemented with 10 mM β-glycerophosphate (Sigma–Aldrich,USA) and $50\,\mu g \cdot mL^{-1}$ ascorbic acid (Sigma–Aldrich,USA) to promote the osteoblastic phenotype. Upon confluence, 7F2 cells were trypsinized and resuspended in medium at a concentration of 3×10^5 cells $\cdot\, mL^{-1}$ which was chosen as to give the maximal response without overly restricting their ability to spread.

Prior to seeding, the sterile unmodified and plasma modified PCL scaffolds were placed in individual wells of a 24-well plate. Then, 7F2 cells were seeded onto scaffolds by adding 1 mL of cell suspension containing 300 000 cells to the top of each scaffold. After 2 h to allow cell attachment, the scaffolds were moved to the new wells to disregard the unattached cells and those that attached to the bottom of the wells. Fresh media (1 mL) was added to each well and the cell–scaffold constructs were maintained in incubation for further examination.

Quantifying the Cell Adhesion Strength and Morphology

The shear flow assay was used for quantifying the strength of cell adhesion on unmodified and plasma modified PCL surfaces with controlled detachment force. The main assumption used in this assay was that the shear stress at the wall ($\tau_w = 6\,\mu Q \cdot wh^{-2}$) was equal to the detachment shear stress at the surface of the cells. Prior to applying the fluid flow, a cell suspension with 1.0×10^5 cells was seeded on the surface of interest and the cells were permitted to settle and attach for 2 h under normal incubation. After the incubation, the sample was placed inside the flow chamber ($25 \times 75 \times 1\,mm^3$) ($w \times L \times h$) and the medium was initiated between the plates with 100–200 mL $\cdot$ min^{-1} for 1 min to obtain the effective shear stress (τ_{50}) at which 50% of the seeded cells were removed compared to the control sample. Following the flow, the attached cells remained on the surface of interest were counted by aB assay (Biosource International, USA).

The morphology of 7F2 mouse osteoblast cells on unmodified and plasma modified 3D PCL scaffold was also examined by SEM to verify the cell adhesion assay. The cell–scaffold constructs were removed from the medium on day 7 and washed with phosphate-buffered saline (PBS; Sigma–Aldrich, USA) three times. The cells were then fixed with 3% gluteraldehyde (Sigma–Aldrich, USA) for 2.5 h at 4 °C. After fixation, the scaffolds were washed with PBS and gradually dehydrated through 50, 70, 80, 90, and 100% ethanol solutions for 30 min each. Following the dehydration, the scaffolds were kept in 4 °C for overnight and next day sputter coated with Plt layer to look under SEM.

Assessment of Cell Proliferation and Differentiation

Quantification of Metabolic Activities

The aB assay (Biosource International, USA) incorporates a fluorometric indicator based on detection of metabolic activity. The amount of fluorescence is directly proportional to the metabolic activity of living cells. The non-toxic aB assay was performed to measure the cell proliferation on unmodified and

oxygen-plasma modified 3D PCL scaffolds ($n = 4$ for each group on each measurement day) at 0, 3, 7, 14, 21, and 28 d after seeding. On the day of characterization, 10% v/v of aB assay solution was added to each well and allowed to incubate for 4 h at incubator condition. After incubation, 800 μL solution of color product was taken out from the wells and put into a 24 well-plate to measure the fluorescence intensity using a microplate fluorometer (Genius, TECAN, USA) at 535 nm excitation and 560 nm emission wavelengths.

Quantification of Alkaline Phosphatase (ALP) Activities

The ALP activities of 7F2 mouse osteoblast cells on PCL scaffolds ($n = 4$ for each group on each measurement day) were assayed with *p*-nitrophenylphosphate (*p*NPP) (Sigma, Cat# N7653) at 14, 21, and 28 d after seeding. On the measurement day, the scaffolds were removed from the medium and washed with PBS twice. Then they were submerged into 1 mL of 1% Triton ×100 solution for an hour. During this period, the solution was agitated several times for the cell lysis. After 1 h, 0.5 mL solution was incubated with 0.5 mL *p*NPP for 45 min at 37 °C. The production of *p*-nitrophenol in the presence of ALP was monitored with microplate fluorometer by the absorbance of 405 nm wavelength. The ALP activity was expressed as unit per cell number.

Quantification of Osteocalcin Release

The amount of osteocalcin synthesized by mouse 7F2 cells was measured by an enzyme-linked immunosorbent assay (ELISA) kit (Biomedical Technologies Inc., Stoughton, MA) at 14, 21, and 28 d after seeding. On characterization day, 25 μL of medium from cell–scaffold constructs were transferred ($n = 4$ for each group on each measurement day) to the 96-well microtiter plates coated with primary antibody. Then, 100 μL of secondary antibody was added into each well and incubated for 18 h at 4 °C. Following the incubation, the samples were aspirated and washed with PBS five times. 100 μL of Streptavidin–Horseradish Peroxidase was added to the wells and incubated again for 30 mins. Subsequently, the samples were washed five times before adding 100 μL of substrate solution into each well and incubating at room temperature, in the dark for 15 min. The reaction was stopped by adding 100 μL of stop solution into the wells and the absorbance was measured immediately at 450 nm. The resulting absorbance values for the samples were converted to osteocalcin concentration ($pg \cdot mL^{-1}$) using a standard curve generated from known concentrations of osteocalcin standard solutions.

Quantification of Calcium Content

The amount of calcium content in the 7F2 mouse osteoblast cell-plasma modified/unmodified scaffold constructs was measured by calcium test kit (Stanbio Laboratory, cat # 0150, Boerne, TX) at 14, 21, and 28 d after seeding. On characterization day, the cell–scaffold constructs ($n = 4$ for each group on each measurement day) were washed twice with PBS and submerged into 0.5 mL 1% Triton X-100 and 0.5 mL trichloroacetic acid at room temperature for 2 h to extract calcium from the mineralized scaffolds. The extracted cell lysate was then centrifuged to get the supernatant for measurement. From each well, a volume of 10 μL supernatant was taken and mixed with 0.5 mL calcium binding reagent (OCPC) and 0.5 mL calcium buffer reagents (2-amino, 2-methyl, 1-propanol) provided with kit. The absorbance of each well was monitored with a microplate fluorometer (Genius, TECAN, USA) at 570 nm. To generate a standard curve, the series calcium dilutions provided by kit were prepared. Then, by using the calibration curve, calcium amounts for each scaffold were calculated. Finally, the calcium amount in each sample was normalized to the total cell number at each point.

Statistical Analysis

The statistical significance of all measurements for unmodified and oxygen-based, plasma modified PCL treatments was determined by analysis of variance (ANOVA) and Tukey post-hoc test at the significance level of less than 0.05 ($p < 0.05$) using SPSS version 14 for Windows software package.

Results

Structural Accuracy of As-fabricated Polycaprolactone (PCL) Scaffolds by Precision Extrusion Deposition (PED) Process

Based on the measured data shown in Table 1, the average strut diameter of ten different scaffolds was 219.66 μm with a standard deviation of 9.14 μm. This corresponds to an accuracy of 90% based on 200 μm as the designed strut diameter. For 200 μm as the designed pore size, the average value is 194.01 μm with a standard deviation of 5.42 μm based on the measurements taken from ten scaffolds. This corresponds to 97% accuracy which is highly precise compared to the other solid freeform scaffold manufacturing techniques. The above results demonstrate that the repeatability, accuracy, and applicability of the PED process for fabrication of complex 3D PCL tissue scaffolds.

Table 1. Measured data of the strut diameter and the pore size of ten scaffolds fabricated by the PED process.

Scaffold	Strut diameter μm	Pore size μm
Scaffold 1	216.21	199.05
Scaffold 2	217.50	195.00
Scaffold 3	210.95	187.50
Scaffold 4	228.28	172.84
Scaffold 5	213.45	212.07
Scaffold 6	206.72	218.88
Scaffold 7	223.10	214.48
Scaffold 8	221.98	183.97
Scaffold 9	238.71	158.28
Scaffold 10	219.74	198.02
Average	219.66	194.01

DOI: 10.1002/ppap.201000009

Effect of Plasma Modification on Polycaprolactone (PCL) Surface Hydrophilicity and Solid Surface Energy

The effect of plasma modification on surface hydrophilicity was measured by the contact angle using different probe liquids on unmodified and plasma modified PCL surfaces, as shown in Table 2. The ± here represents the standard deviation with $n = 4$ for each probe liquids.

The results of the contact angle measurement indicated showed that the measured contact angles decreased significantly after the plasma modification. That means the increasing surface hydrophilicity as result of the plasma surface treatment. The measured contact angles were then used to calculate the polar, dispersive, and total surface energy of PCL before and after the plasma modification. The change in total surface energy (σ_s) of PCL and its polar (σ_s^P) and dispersive (σ_s^D) components after plasma modification was calculated by the Owens–Wendt's method. The variation in the total, polar, and dispersive solid surface energy of unmodified and plasma modified PCL are presented in Figure 2. Figure 2 shows that total surface energy of PCL increases from 39 $mN \cdot m^{-1}$ for the unmodified PCL to 54 $mN \cdot m^{-1}$ for 1-min plasma modified, 51 $mN \cdot m^{-1}$ for 3-min plasma modified and 49 $mN \cdot m^{-1}$ for 5-min plasma modified PCL samples. Compared to the unmodified PCL, the plasma modification does increase the total surface energy, particularly for the polar component though there was no significant difference for the total surface energy in terms of the modification time.

Effect of Plasma Surface Modification on Polycaprolactone (PCL) Surface Chemistry

The change in surface chemistry on PCL sample before and after oxygen-based plasma modification was determined by XPS. In order to identify the changes in fraction of various functional groups on modified PCL samples, high resolution scans for C1s, O1s, Si2s, Si2p, and N1s were taken. Then, C1s spectra were deconvoluted into four peaks which are C1 at 285 eV, C2 at 286.4 eV, C3 at 288.9 eV, and C4 at 287.8 eV.

Table 2. The static contact angle data of probe liquids on unmodified and modified PCL surfaces.

	Static contact angle (°)		
	Ultra pure water	**Glycerol**	**Diiodomethane**
Unmodified	58 ± 6	71 ± 3	34 ± 8
1-min modified	34 ± 1	38 ± 5	27 ± 4
3-min modified	41 ± 1	38 ± 1	31 ± 6
5-min modified	44 ± 3	43 ± 3	30 ± 5

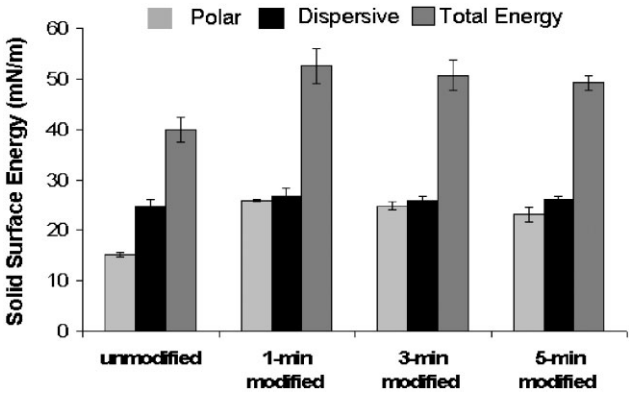

Figure 2. The polar, dispersive, and total surface energy ($mN \cdot m^{-1}$) for unmodified, 1, 3, and 5-min oxygen-based plasma modified PCL surface.

Figure 3 shows the deconvoluted C1s peak survey XPS spectra of unmodified and plasma modified PCL at 1-, 3-, and 5-min.

Figure 3 shows that with the plasma modification the surface chemistry and the fraction of functional groups on the surface were both changed. The functional groups contains carbon atoms with two oxygen bonds like carbonyl group peaking at 287.8 eV was introduced to the PCL surface after the plasma modification without any exception. In order to observe changes in functional groups, the area under the C1, C2, C3, and C4 peaks were calculated. The results are given in Table 3.

Based on the results shown in Figure 3 and Table 3, we observed that after the plasma modification, the percentage of carbon–carbon bonds (C—C) was decreased (Table 3). This can be attributed to cleavage of C—C, C—H bonds on the backbone of PCL and introduction of new functional groups. We also found that the fraction of oxygen containing functional groups was also changed after the plasma modification. The amount of total oxygen containing functional groups (hydroxyl, carboxyl, and carbonyl) was highest on 1-min plasma modified PCL with a value of 46.78, 32.42% for 3-min plasma modified and 31.95% for 5-min modified PCL samples, comparing t 31.07% for unmodified PCL.

Effect of Plasma Surface Modification on Polycaprolactone (PCL) Surface Topography

The changes in PCL surface structure and the topography after the plasma modifications were measured and imaged by using AFM. The results of the RMSR for unmodified and plasma modified PCL are given in Table 4. Three different locations on each sample were examined by AFM. The ± represents the standard deviation of surface roughness for each sample. The AFM phase images (3D) for unmodified, 1-, 3-, and 5-min plasma modified PCL are also given in Figure 4.

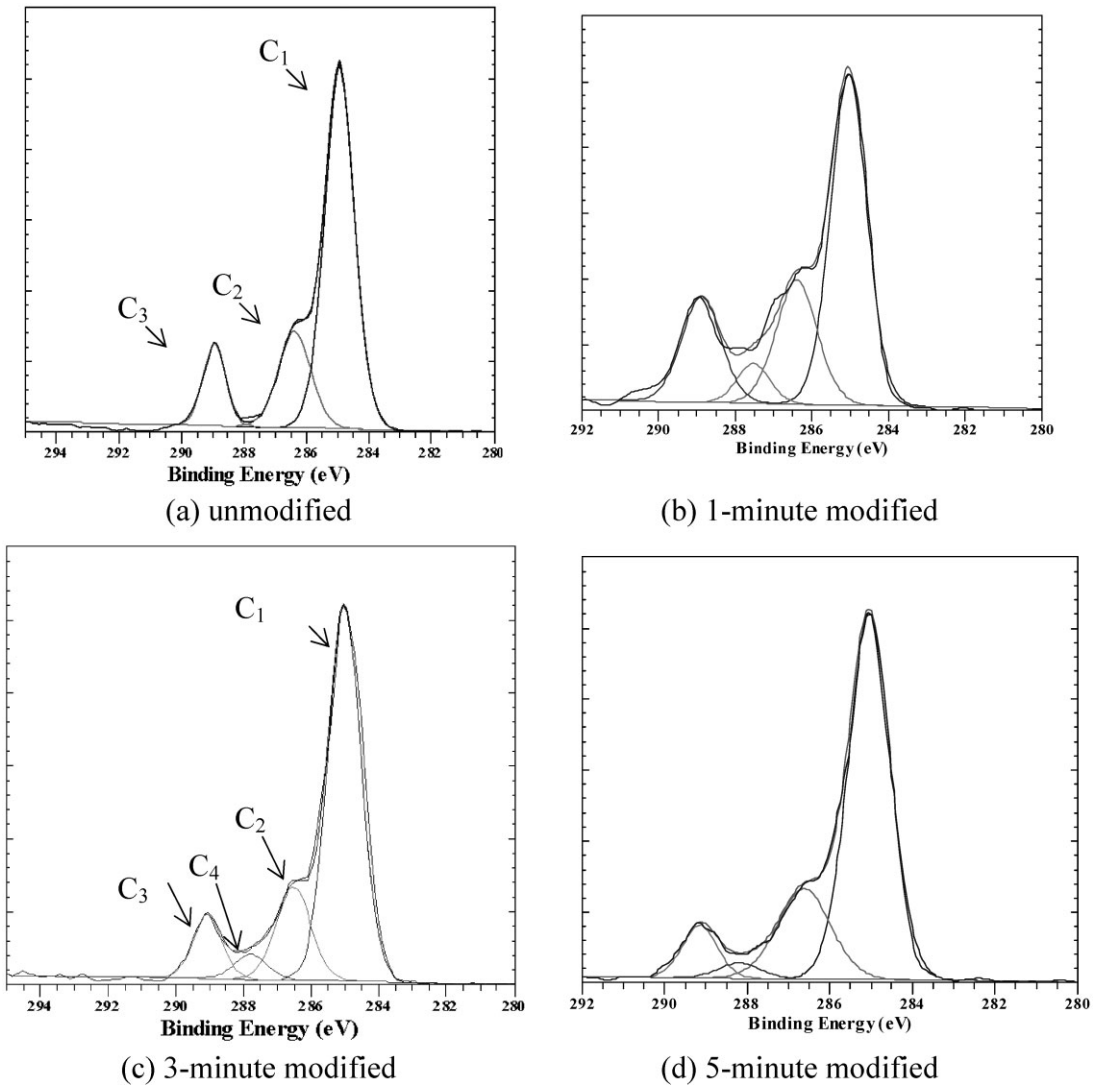

Figure 3. The deconvoluted C1s XPS spectra of PCL surface (a) unmodified, (b) 1-min modified, (c) 3-min modified, (d) 5-min modified.

The roughness measurements and the height data images shown in Figure 4 suggest that the plasma modification increases the PCL surface roughness. After 1-min plasma modification, the surface roughness was increased 75% to 72 ± 4 nm compared to unmodified PCL (41 ± 8 nm as shown in Figure 4a and Table 3), and 150 ± 12 nm for 3-min plasma modification time. With the prolonged plasma modification time, the surface roughness started to decrease to 50 ± 6 for 5-min plasma modification, suggesting the etching effect is more dominant for prolonged plasma exposure.

Table 3. The fraction of C1s components on PCL surface.

Modification Type	C1 (%) 285 eV	C2 (%) 286.4 eV	C3 (%) 288.9 eV	C4 (%) 287.8 eV
Unmodified	68.93	19.53	11.54	–
1-min modified	53.22	22.61	5.72	18.45
3-min modified	67.58	17.81	10.24	4.37
5-min modified	68.05	21.06	8.06	2.83

Effect of Plasma Surface Modification on Cell–Scaffold Interaction

Cell Adhesion and Morphology

The quantitative data of the cell attachment was obtained by applying a parallel plate shear flow assay for seven different plasma modifications time: 0, 0.5, 1, 2, 3, 5, and 7 min. Figure 5 shows the fluorescence intensity of attached

DOI: 10.1002/ppap.201000009

Table 4. Surface root mean square roughness (RMSR) for unmodified and modified PCL.

	Unmodified	1-min modified	3-min modified	5-min modified
RMSR (nm)	41 ± 8	72 ± 4	150 ± 12	50 ± 6

cells on unmodified (0 min) as well as 0.5, 1, 2, 3, 5, and 7 min plasma modified PCL samples under a 27 dynes $\cdot$ cm^{-2} shear stress. The results suggest that the 3-min plasma modification results in the maximum retention of cells at the same detachment force compared to the other unmodified and modified samples. It is clear to say that the 3-min plasma modification will yield the greatest surface roughness (Figure 4) and the cell retention (Figure 5). Therefore, we will use 3-min as the plasma modification time for the following cellular study (metabolic activity and differentiation).

The positive effect of plasma modification on cell attachment was also evaluated by scanning electron microscopy (SEM). Figure 6 shows the low and high magnification of SEM micrographs for 7F2 mouse osteoblast cells incubated on unmodified and modified PCL scaffolds on day 7. In low magnification (Figure 6A), one can only observe individual small number cells scattered over the unmodified PCL scaffolds. Figure 6B shows that the cells on 3-min plasma modified PCL samples started to cover the

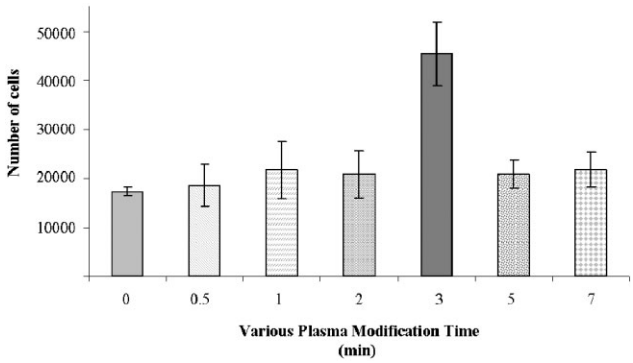

Figure 5. The fluorescence intensity of attached cells on various times (0, 0.5, 1, 2, 3, 5, and 7 min) plasma modified PCL scaffolds.

struts of the scaffold with higher number. The morphology of cells on scaffolds strut could be examined more easily in a high magnification of SEM micrographs. For example, cells were preserved un-elongated round shape on the unmodified PCL scaffolds (Figure 6C), while exhibited elongated morphology on scaffold struts with a high degree of spreading on 3-min plasma modified PCL scaffolds (Figure 6D).

Cell Metabolic Activity and Differentiation

The metabolic activity of 7F2 mouse osteoblast cells on unmodified and 3-min plasma modified 3D PCL scaffolds

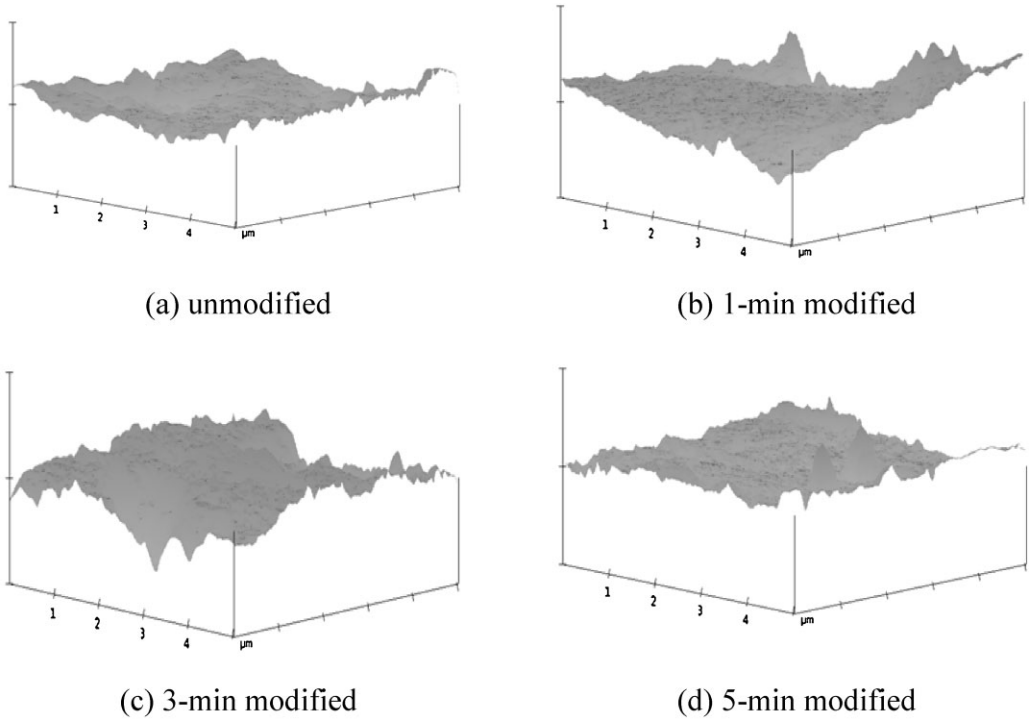

Figure 4. AFM surface topography height data image for PCL samples: (a) Unmodified, (b) 1-min modified, (c) 3-min modified, and (d) 5-min modified.

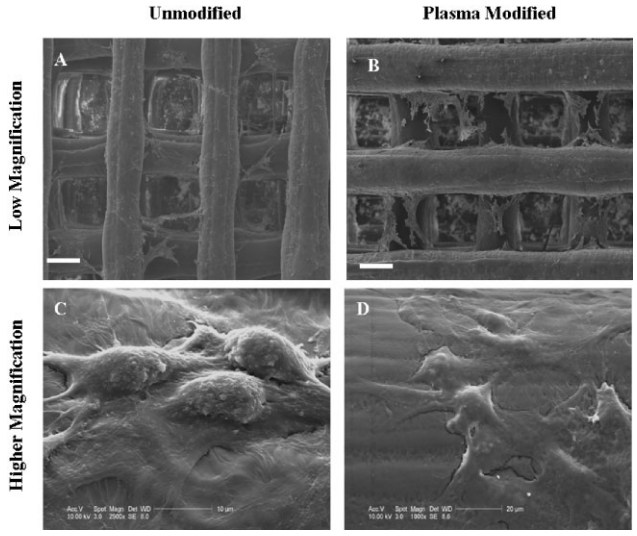

Figure 6. The SEM micrographs of cells on unmodified and 3-min oxygen-based plasma modified PCL scaffolds at day 7. Cells on (A) unmodified scaffolds with low magnification (B) 3-min plasma modified scaffolds with low magnification, (C) unmodified scaffolds with high magnification, (D) 3-min plasma modified scaffolds with high magnification (scale bars represent 200 μm).

were measured by aB assay. The measured metabolic activity of cells on scaffolds at day 0, 3, 7, 14, 21, and 28 are presented in Figure 7. As shown in the figure, there was an increase in metabolic activity on both modified and unmodified scaffolds until day 7. After 7 d cell culture, cells on 3-min plasma modified scaffolds had higher metabolic activity compared to unmodified scaffolds. However, on day 14 the cell population began to level off, and less cell metabolic activity found in day 21 and day 28 due to the saturation of the cells.

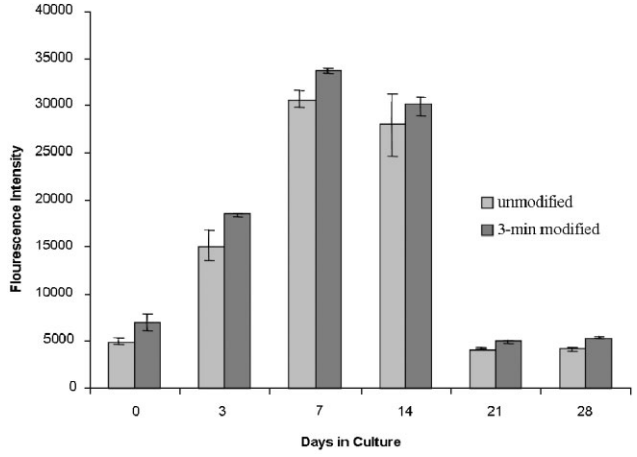

Figure 7. The fluorescence intensity of cells on 3-min plasma modified and unmodified PCL scaffolds up to 28 d (error bars represent ± standard deviation with $n = 4$ for each group).

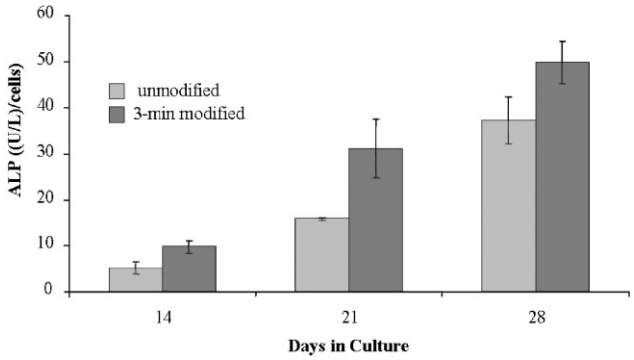

Figure 8. ALP activity on plasma modified and unmodified PCL scaffolds over 28 d ($n = 4$ for each group and each measurement day).

It is apparent that the metabolic activity which is corresponding to cell proliferation increased steadily up to day 7 and then deceased afterwards. We believe that this was because the number of cells reached to a saturation stage, and partially the 7F2 mouse osteoblast cells started differentiation.[25] We further quantified the differentiation in the unmodified and 3-min modified samples by evaluating ALP and osteocalcin and calcium mineralization differentiation markers on day 14, 21, and 28.

Alkaline Phosphatase (ALP) Activities

Alkaline Phosphatase (ALP) activity of 7F2 mouse osteoblast cells on unmodified and plasma modified PCL scaffolds were examined by p-nitrophenylphosphate (*p*NPP) on day 14, 21, and 28. The results given in Figure 8 shows that ALP activity reached detectable amount in culture at day 14. Both unmodified and plasma modified scaffold–cell constructs expressed ALP activity which increased from day 14 to day 28. The 7F2 mouse osteoblast cells seeded on 3-min plasma modified scaffolds expressed significantly higher levels of ALP activity compared to the unmodified scaffolds on each measurement day.

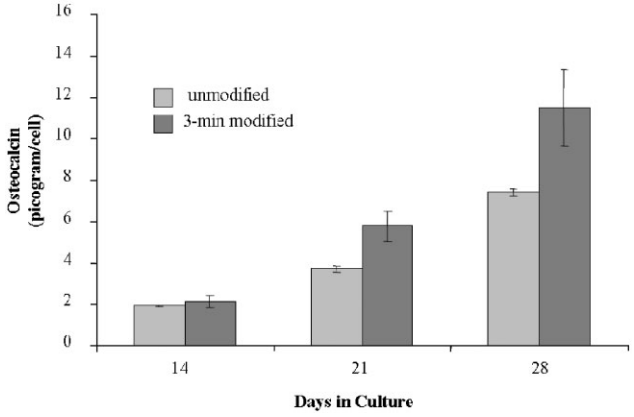

Figure 9. Amount of osteocalcin protein secreted up to 28 d ($n = 4$ for each group and each measurement day).

DOI: 10.1002/ppap.201000009

Osteocalcin Secretion

The amount of osteocalcin secretion at day 14, 21, and 28 are shown in Figure 9. The results suggest that up to day 14 there was no significant difference in osteocalcin amount between the unmodified and the plasma modified scaffolds. However, with the prolonged culture time the osteocalcin secretion was increased in both unmodified and plasma modified PLC scaffolds, and the increase was greater for 3-min plasma modified PCL scaffold compared to unmodified ones. This also means that that 7F2 mouse osteoblast cells on 3-min plasma modified PCL scaffolds differentiate faster than the cells on unmodified PCL scaffolds.

Calcium Mineralization

The characterization of calcium deposition for 7F2 mouse osteoblast cells on the unmodified and plasma modified 3D PCL scaffolds at 14, 21, and 28 d is shown in Figure 10. The mineralization formation increased significantly in plasma modified PCL scaffolds compared to the unmodified PCL scaffolds. Highest mineralization was obtained on day 28 on 3-min plasma modified PCL scaffolds. In addition to quantitative analysis in mineralization, qualitative measurement was done by SEM micrographs given in Figure 11. The SEM micrographs in Figure 11D and F proved that 7F2 mouse osteoblast cells on the plasma modified scaffolds have significantly higher mineralized matrix deposition and extracellular matrix (ECM) formation compared to the unmodified scaffolds.

In Figure 11, the long-term 7F2 cells behavior on unmodified and 3-min plasma modified 3D PCL scaffolds were characterized by SEM micrographs of scaffolds on day 14, 21, and 28. Starting from day 14, the cells on plasma modified scaffolds appeared to bridge over the pores (Figure 11B) and to cover the struts before forming circular regions around the pores (Figure 11D). On day 28, the calcium mineralization was found to spread over the plasma modified PCL scaffolds (Figure 11E). The SEM micrographs in Figure 11E and F showed that the cells on 3-min plasma modified PCL scaffolds produced more mineralized matrix, compared to unmodified PCL scaffolds. As matter of fact, the cells on unmodified scaffolds did not show significant cellular functions such as ECM formation and throughout the incubation periods (Figure 11A, C, and E). The SEM micrographs also further confirmed that the differentiation of 7F2 mouse osteoblast cells had been enhanced by applying a 3-min oxygen-based plasma modification to the PCL scaffolds, compared to unmodified PCL samples.

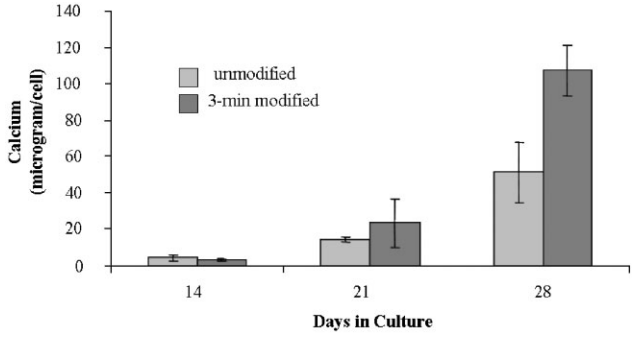

Figure 10. Calcium content produced by cells cultured on 3D PCL scaffolds up to 28 d ($n = 4$ for each group and each measurement day).

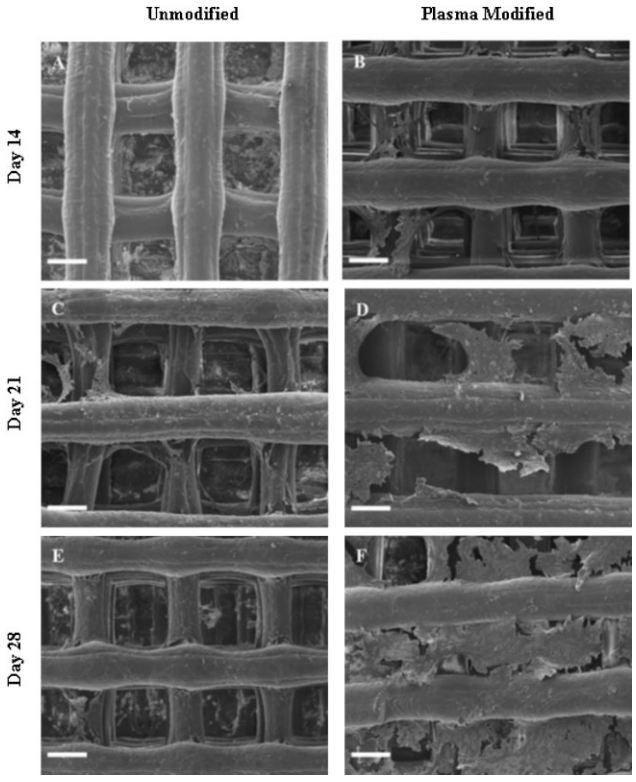

Figure 11. The SEM micrographs of 7F2 mouse osteoblast cells on unmodified and 3-min oxygen-based plasma modified PCL scaffolds after incubation 14, 21, and 28 d. Cells on (A) unmodified scaffolds on day 14 (B) plasma modified scaffolds on day 14 (C) unmodified scaffolds on day 21 (D) plasma modified scaffolds on day 21 (E) unmodified scaffolds on day 28 (F) plasma modified scaffolds on day 28 (Scale bars represent 200 μm).

Discussion

One of the ultimate goals of bone tissue engineering is to create osteoblast–scaffold constructs for bone tissue replacement. It is known from *in vivo* studies that the differentiation of 7F2 mouse osteoblast cells is the main event toward to bone tissue regeneration.[26,27] Therefore the current study may provide a useful approach of using

plasma modification to enhance osteoblast cells proliferation and differentiation. In conjunction with the enabling PED process, one can arrive at desirable 3D tissue scaffolds with well-defined internal architecture (fabricated through PED process) and ideal surface properties (through plasma modification). Results in this study strongly suggest that the plasma modification enhances an overall behavior of the cell–scaffold interaction. The 3-min plasma modification increases cell adhesion, proliferation, and differentiation, specifically, increase the cell adhesion strength (Figure 5 and 6), the metabolic activities (Figure 7) and up-regulated the osteoblast specific gene expression such as ALP activity (Figure 8), osteocalcin secretion (Figure 9), and the matrix mineralization (Figure 11).

The surface characterization by the contact angle measurement and by the Owens–Wendt method demonstrated that the surface hydrophilicity and total surface energy have been increased with plasma modification (Table 1 and Figure 2). The major contributor in energy increment was polar component of the surface energy. Compared to dispersive component, polar component increased with the plasma modification. This might be explained by the changes in surface chemistry and topography after plasma exposure. The surface chemistry data (Figure 3) from XPS showed that the chemical structure of PCL surface was altered by the plasma modification. The remarkable alteration was observed on 1-min plasma modified PCL surface toward increment in total oxygen content of the surface. Particularly, compared to 3- and 5-min plasma modified PCL, 1-min had the highest amount of carbon atoms with two bonds oxygen such as carbonyl (C=O) groups on the surface (Table 3). In addition to surface chemistry, surface topography was also measured and pictured after plasma modification through AFM. The data (Table 4 and Figure 4) suggested that plasma modification increased the surface roughness. The highest increment was observed on 3-min plasma modified samples from 41 ± 8 nm for unmodified PCL to 150 ± 12 nm surface roughness. Both from chemistry and roughness data, it was observed that after 3-min of plasma exposure with the prolonged modification time; the surface properties tend to become its native conditions. For instance, for 5-min modified PCL, the oxygen content of the surface and surface roughness were decreased to its original amount as before plasma modification.

In order to identify the optimal plasma modification time for increased cell–scaffold interaction, the cell adhesion assay were carried out. The cell adhesion result (Figure 5) showed that 3-min plasma modification had the greatest retention of cells at the same detachment force compared to 0, 0.5, 1, 2, 5, and 7 min plasma modified samples. This might be explained with the dominant effect of increased surface roughness on osteoblast attachment. Because if the increased oxygen content of the surface increased the cell adhesion, we would have expected that 1-min plasma modified PCL had the highest cell number based on XPS data. Based on cell adhesion data, the optimal plasma modification time for extended cellular study (proliferation and differentiation) was chosen as 3-min. The SEM micrographs of cell morphology (Figure 6) and the proliferation assay (Figure 7) demonstrated the enhanced cell attachment and proliferation on 3-min modified PCL scaffold. The SEM micrographs on day 7 showed that the cells on the 3-min plasma modified PCL scaffolds attached and elongated much better than the unmodified samples (Figure 6). The osteoblast proliferation on PCL scaffolds was also improved by plasma modification (Figure 8). Compared to unmodified scaffolds, the cell number on 3-min plasma modified PCL scaffolds was higher during the proliferation phase of 7F2 (after 7 d of cell culture).

We believe that the improved cell adhesion might be the reason for an increased cell metabolic activity because most of the mammalian cells including osteoblasts need to spread out before proliferation. The inadequate spreading due to poor adhesion can inhibit the proliferation and can delay the differentiation.[28] We further believe that after plasma modification the increased surface roughness in conjunction with increased fraction of oxygen functional groups on the surface might be the reasons in enhanced osteoblast attachment and proliferation. Because cell adhesion is mediated by cells' transmembrane receptors called integrin. When cells approaches to the biomaterials first interaction was between cells' receptor (integrin) and the adsorbed protein layer on the biomaterial surface. The amount of protein adsorption is affecting the bonding strength of integrin.[29,30] In light of previous studies, it is known that the adsorption behavior of the surface can be altered by changing the surface roughness and chemistry of the biomaterials. By increasing surface roughness and increased surface polarity, the higher amount of protein can be adsorbed on the surface which will lead to strong cell-matrix adhesion.[31–32]

The effect of enhanced cell adhesion through plasma modification on latter stage of osteoblast were examined by differentiation markers; ALP, osteocalcin, and calcium mineralization. The results showed that starting from day 14, the metabolic activity which corresponds on both unmodified and modified PCL scaffolds started to level off (Figure 7). The decrease in incremental cell number after day 7 and increase in expression of osteoblast phenotype shown in Figure 8 were the consequence of initial cell differentiation. It was known that the developmental sequence of osteoblast cells have three principle periods: proliferation, ECM maturation, and mineralization.[33] A gene expression associated with the matrix maturation is induced when the cell proliferation is down-regulated, and then the mineralization occurs. A reciprocal and functionally coupled relationship between the decline in prolifera-

DOI: 10.1002/ppap.201000009

tion activity and the subsequent induction of matrix maturation and mineralization was supported by enhanced expression of ALP immediately following the proliferation period, and later, an increased expression of osteocalcin at the onset of mineralization.[25] The ALP activity (Figure 8), osteocalcin secretion (Figure 9), and calcium mineralization (Figure 10) data demonstrated that osteoblast cells on 3-min plasma modified PCL scaffolds had higher expression of ALP activities, osteocalcin secretion, and calcium mineralization compared to counterparts on unmodified scaffolds. Results presented in Figure 11 further indicate that after day 21 the amount of mineralized calcium on plasma modified PCL scaffolds was significantly higher than the unmodified ones. The amount of calcium mineralization correlates to the level of tissue mineralization, with greater calcium levels associated with further differentiation.[33–35]

Conclusion

This study demonstrates that an oxygen-based plasma modification can be applied to alter the physicochemical properties of 3D PCL scaffolds and to improve the mouse osteoblast cells attachment, proliferation, and osteoblastic differentiation. The contact angle measurement, total solid surface energy, surface chemistry, and roughness results revealed that oxygen-based plasma modification increased surface hydrophilicity, total surface energy, total amount of oxygen containing groups, and the surface roughness. The effect of oxygen-based plasma modification on attachment, proliferation, and osteoblastic differentiation were examined by, shear flow assay, aB assay, SEM, and osteoblastic differentiation markers. The strength of osteoblast adhesion was found to be greatest on the 3-min plasma modified PCL compared to cell attachment on 0, 0.5, 1, 2, 5, and 7 min plasma modified PCL. The SEM micrograph of cells taken at day 7 also confirmed the improved cell attachment by elongated and stretched cell morphology on 3-min plasma modified PCL scaffolds. We observed a positive effect of plasma modification on 7F2 proliferation on 3D PCL scaffolds till the beginning of the osteoblastic differentiation stage (day 14). With the production of ECM the cell number decreased and ALP activity, osteocalcin protein secretion, and calcium mineralization were initiated. The higher ALP activity and osteocalcin secretion were detected from the 7F2 cells on 3-min plasma modified PCL surface compared to unmodified samples. The calcium mineralization and SEM micrographs data also showed that there was a higher mineralized matrix deposition on 3-min plasma modified PCL scaffolds compared to unmodified scaffolds. These results suggest through 3-min plasma modification we can accelerate the differentiation phase of osteoblast through improving cell–scaffold interaction.

Received: January 25, 2010; Revised: September 15, 2010; Accepted: November 15, 2010; DOI: 10.1002/ppap.201000009

Keywords: osteoblast differentiation; oxygen plasma surface modification; polycaprolactone; surfaces; three-dimensional scaffolds; tissue engineering

[1] J. Zeltinger, J. K. Sherwood, D. A. Graham, R. Mueller, L. Griffith, *Tissue Eng.* **2001**, *7*, 557.
[2] I. Zein, D. W. Hutmacher, K. C. Tan, S. H. Teoh, *Biomaterials* **2002**, *23*, 1169.
[3] V. Maquet, R. Jerome, Design of Macroporous-biodegradable Polymer Scaffolds for Cell Transplantation, in: *Porous Materials for Tissue Engineering*, D. Liu, V. Dixit, Eds., Trans. Tech. Publications, Totton, Hampshire, UK 1997, pp. 15–42.
[4] M. C. Wake, C. W. Partick Jr, A. G. Mikos, *Cell Transplant.* **1994**, *3*, 339.
[5] A. G. Mikos, G. Sarakinos, L. A. Czerwonka, Y. Bao, R. Langer, *Polymer* **1994**, *35*, 1068.
[6] B. D. Ratner, A. S. Hoffman, F. J. Schoen, J. E. Lemons, Eds., "*Biomaterials Science: An Introduction to Materials in Medicine*" Academic Press, San Diego 1996.
[7] R. A. Jain, *Biomaterials* **2000**, *21*, 2475.
[8] D. W. Hutmacher, T. Schantz, I. Zein, K. W. Ng, S. H. Teoh, K. C. Tan, *J. Biomed. Mater. Res.* **2001**, *55*, 203.
[9] E. D. Yildirim, R. Besunder, S. Guceri, F. Allen, W. Sun, *Virtual Phys. Prototyping* **2008**, *3*, 199.
[10] L. Shor, R. Chang, S. Güçeri, J. Gondon, Q. Kang, L. Hartsock, Y. An, W. Sun, *Biofabrication* **2009**, *1*, 1.
[11] X. H. Liu, P. X. Ma, *Ann. Biomed. Eng.* **2004**, *32*, 477.
[12] H. Zhang, C. Y. Lin, S. J. Hollister, *Biomaterials* **2009**, *30*, 25.
[13] F. Migneco, Y. C. Huang, R. K. Birla, K. Ravi, S. J. Hollister, *Biomaterials* **2009**, *30*, 33.
[14] W. W. Hu, Y. Elkasabi, H. Y. Chen, Y. Zhang, J. Lahann, S. J. Hollister, P. H. Krebsbach, *Biomaterials* **2009**, *30*, 29.
[15] L. Shor, S. Güçeri, M. Gandhi, W. Sun, *Biomaterials* **2007**, *28*, 35.
[16] H. U. Lee, Y. S. Jeong, S. Y. Jeong, S. Y. Park, J. S. Bae, H. G. Kim, C. R. Cho, *Appl. Surf. Sci.* **2008**, *254*, 5700.
[17] Z. Y. Cheng, S. H. Teoh, *Biomaterials* **2004**, *25*, 1991.
[18] A. R. Sarasam, R. K. Krishnaswamy, S. V. Madihally, *Biomacromolecules* **2006**, *7*, 1131.
[19] K. S. Tiaw, S. W. Goh, M. Hong, Z. Wang, B. Lan, S. H. Teoh, *Biomaterials* **2005**, *26*, 763.
[20] B. Pignataro, E. Conte, A. Scandurra, G. Marletta, *Biomaterials* **1997**, *18*, 1461.
[21] E. D. Yildirim, H. Ayan, V. N. Vasilets, A. Fridman, S. Guceri, G. Friedman, W. Sun, *Plasma Process. Polym.* **2008**, *5*, 397.
[22] D. Pappas, A. Bujanda, J. Orlicki, R. Jensen, *Surf. Coatings Technol.* **2008**, *203*, 830.
[23] F. Arefi-Khonsari, M. Tatoulian, F. Bretagnol, O. Bouloussa, F. Rondelez, *Surf. Coatings Technol.* **2005**, *200*, 14.
[24] F. Wang, L. Shor, A. Darling, S. Khalil, W. Sun, S. Güçeri, A. Lau, *Rapid Prototyping J.* **2004**, *10*, 1.
[25] T. A. Owen, M. Aronow, V. Shalhoub, L. M. Barone, L. Wilming, M. S. Tassinari, M. B. Kennedy, S. Pockwinse, J. B. Lian G. S. Stein, *J. Cell. Physiol.* **1990**, *143*, 420.
[26] Z. Gugala, S. Gogolewski, *Biomaterials* **2004**, *25*, 2299.
[27] Z. Gugala, S. Gogolewski, *Biomaterials* **2004**, *25*, 2341.

[28] S. Wu, "*Polymer Interface and Adhesion*", Marcell Dekker Inc., New York 1982.
[29] A. J. Garcia, *Biomaterials* **2005**, *26*, 7525.
[30] B. G. Keselowsky, D. M. Collard, A. J. Garcia, *Proc. Natl. Acad. Sci. USA* **2005**, *102*, 5953.
[31] C. J. Wilson, R. E. Clegg, D. I. Leavesley, M. J. Pearcy, *Tissue Eng.* **2005**, *11*, 1.
[32] S. B. Kennedy, N. R. Washburn, C. G. Simon, E. J. Amis, *Biomaterials* **2006**, *27*, 3817.
[33] K. Anselme, *Biomaterials* **2000**, *21*, 667.
[34] K. Anselme, M. Bigerelle, *Biomaterials* **2006**, *27*, 1187.
[35] H. L. Holtorf, J. A. Jansen, A. G. Mikos, *Biomaterials* **2005**, *26*, 6208.

DOI: 10.1002/ppap.201000009